arXiv:1306.5865v3 [astro-ph.HE] 17 Oct 2013

Hints of an axion-like particle mixing in the GeV gamma-ray blazar data?

Olga Mena[a] **and Soebur Razzaque**[b]

[a]*IFIC, Universidad de Valencia-CSIC, E-46071, Valencia, Spain*
[b]*Department of Physics, University of Johannesburg, PO Box 524, Auckland Park 2006, South Africa*
E-mail: `omena@ific.uv.es`, `srazzaque@uj.ac.za`

ABSTRACT: Axion-Like Particles (ALPs), if exist in nature, are expected to mix with photons in the presence of an external magnetic field. The energy range of photons which undergo strong mixing with ALPs depends on the ALP mass, on its coupling with photons as well as on the external magnetic field and particle density configurations. Recent observations of blazars by the *Fermi Gamma-Ray Space Telescope* in the 0.1–300 GeV energy range show a break in their spectra in the 1–10 GeV range. We have modeled this spectral feature for the flat-spectrum radio quasar 3C454.3 during its November 2010 outburst, assuming that a significant fraction of the gamma rays convert to ALPs in the large scale jet of this blazar. Using theoretically motivated models for the magnetic field and particle density configurations in the kiloparsec scale jet, outside the broad-line region, we find an ALP mass $m_a \sim (1-3) \cdot 10^{-7}$ eV and coupling $g_{a\gamma} \sim (1-3) \cdot 10^{-10}$ GeV^{-1} after performing an illustrative statistical analysis of spectral data in four different epochs of emission. The precise values of m_a and $g_{a\gamma}$ depend weakly on the assumed particle density configuration and are consistent with the current experimental bounds on these quantities. We apply this method and ALP parameters found from fitting 3C454.3 data to another flat-spectrum radio quasar PKS1222+216 (4C+21.35) data up to 400 GeV, as a consistency check, and found good fit. We find that the ALP-photon mixing effect on the GeV spectra may not be washed out for any reasonable estimate of the magnetic field in the intergalactic media.

KEYWORDS: axions, active galactic nuclei, magnetic fields, gamma ray   detectors.

Contents

1. Introduction

Axion-photon transition in an external static electric or magnetic field [1, 2, 3] is generally referred to as the Primakoff effect, originally proposed for neutral pion production by the interaction of a photon with atomic nucleus. Axion-like particles (ALPs, see the recent review of Ref. [4]) , which are a generalization of the QCD axions [5], are characterized by these two photon vertex interactions. Strong theoretical motivation for the existence of ALPs arises from string theory compactifications, which provide the so-called *axiverse* scenarios, with plenty of candidates for ALPs, see Refs. [6, 7, 8, 9].

The conversion between photons and ALPs is determined by the ALP-photon coupling $g_{a\gamma}$, and it has been extensively studied in the context of astrophysical sources in order to search for the hypothetical ALPs in the optical to X-ray data. These searches exclude large regions in the m_a–$g_{a\gamma}$ parameter space of the ALP mass and its coupling to photons (see e.g. Ref. [10, 11] for recent bounds). In particular, axion energy losses in stars have provided strong constraints in the ALP parameter space [12]. The emission of ALPs would decrease the duration of the Helium burning (the Horizontal Branch, HB, stage), and therefore the number of counts in observations of galactic globular clusters. The authors of Ref. [11], using massive stars, have recently confirmed and sharpened the constrain on the ALP photon mixing parameter $g_{a\gamma} < (0.8 - 1) \cdot 10^{-10}$ GeV^{-1}. Future terrestrial based ALP searches, as those from the ALPS II experiment, are also highly promising [13].

Search for ALPs in the γ-ray data from astrophysical sources is being widely discussed in recent years. Conversion of γ rays to very light ALPs has been proposed to take place at the sources such as the Active Galactic Nuclei (AGNs) [14, 15] and Gamma-Ray Bursts (GRBs) [16]; or in the intergalactic space [17, 18, 19]; and in the Milky Way [20]. Depending on the magnetic field strength of the medium in which the γ rays propagate, conversion to ALPs could be possible for $m_a \lesssim 10^{-6}$ eV.

In this paper we report on our search for ALPs in the GeV γ-ray data from the best-studied blazar[1] in the GeV band, namely the flat-spectrum radio quasar (FSRQ) 3C454.3 at a redshift $z = 0.859$. *Fermi*-Large Area Telescope (LAT) monitored this blazar daily in its regular survey mode and detected an extraordinary 5 day outbursts from 2010 November 17th to 21st [21]. The spectra of γ rays at different epochs from 2010 September 1st to December 13th period, which includes the 5 day outbursts, show a break or deviation of the spectra (softening) from a single power law in the 1–10 GeV range. We have fitted these spectra and their breaks using an ALP-photon mixing model for the γ-ray propagation in the magnetized jet that extends to kiloparsecs ($1\,\mathrm{kpc} = 3 \cdot 10^{21}$ cm) outside the blazar's Broad-Line Region (BLR) at $\lesssim 10^{18}$ cm from the central super-massive black hole[2], assuming that the observed γ rays are emitted from the outer edge of or beyond the BLR. From our fits we have extracted the values for m_a and $g_{a\gamma}$, together with the environmental (magnetic field and particle density) and spectral (power-law index and normalization at production) parameters that best describe the data.

As a consistency check, we have also fitted *Fermi*-LAT and MAGIC data of another FSRQ PKS1222+216 at redshift $z = 0.432$, using the same m_a and $g_{a\gamma}$ values obtained from fitting 3C454.3 data but varying the environmental and spectral parameters. PKS1222+216 data obtained by *Fermi*-LAT [22] and MAGIC [23] during 2010 June have less constraining power for the ALP parameters.

The plan of the paper is the following. We discuss in detail our ALP-photon mixing model set-up for the blazar jet in Sec. 2. In Secs. 3 and 4 we fit γ-ray data of 3C454.3 and PKS1222+216 using our formalism and report results. We discuss our results and conclude in Sec. 5.

2. ALP-photon mixing model for blazar jets

The γ-ray emission region for blazars is a hotly-debated topic. Observations of rapid variability of fluxes at very-high energy (VHE, $\gtrsim 100$ GeV) γ rays from several different blazars on time scales as short as $\sim few$ minutes [24, 25, 23] imply that the γ-ray emitting region must be very compact, a size scale of only $\sim 10^{14}$ cm from the causality condition. In case the whole jet cross-section is the γ-ray emitting region, then the above size scale also corresponds to an estimate of the radius from the central super-massive black hole and is well below the BLR. On the other hand, multi-wavelength observations that "trace" the propagation of electromagnetic, from radio to γ rays, emission region in a blazar jet strongly suggest that the γ-ray emission region is at or beyond the BLR [26]. Production of γ rays from a large scale jet also helps to avoid inevitable $\gamma\gamma$ pair production by VHE photons with low-energy photons at small radii. Rapid variability of VHE flux in this case is explained as emission from small scale regions embedded within a large scale jet, i.e., jets within a jet [27]. For our modeling we have adopted this latter scenario of the γ-ray production region at a radius at the outer edge of the BLR or slightly beyond.

---

[1]A small fraction of AGNs with their relativistic jets pointing towards our line of sight.

[2]This region is filled with dense clouds which emit strong atomic transition lines and the distance scale from the central black hole depends on the particular line luminosity.

We assume that GeV γ rays are emitted from a radius $R \approx 10^{18}$ cm from the central super-massive black hole and propagate through the kpc scale jet. The configuration of the magnetic field and the particle density in the AGN jets are not fully known yet. It is expected from the flux-freezing condition that the magnetic field parallel (poloidal) and perpendicular (toroidal) to the jet velocity scale with the jet radius, respectively, as $\propto R^{-2}$ and $\propto R^{-1}$ [28]. Thus, at large radii the toroidal or transverse component should dominate. It was also argued sometime ago that Poynting flux in the AGN jet produce a toroidal magnetic field $B \simeq 0.4 f^{1/2} (L_w/10^{46}\,\mathrm{erg\,cm^{-1}})(R/10^{18}\,\mathrm{cm})$ G, which provides magnetic pressure to confine the BLR clouds [29]. Here L_w is the luminosity of a relativistic wind in the jet and f is the fraction of the wind energy in the Poynting flux. Reverberation measurements of the BLR clouds suggest a power-law profile, R^{-s}, of particle density in the jet with $1 \lesssim s \lesssim 2$ being favored [30]. The profile could be steeper (e.g. $s \sim 3$) outside the BLR, which has a particle density $\gtrsim 10^{10}$ cm^{-3} [30].

For our ALP-photon mixing model in the jet of the blazar 3C454.3, motivated by the above discussion, we adopt the following transverse magnetic field and particle (electron) density profiles

$$B_T = \phi \left(\frac{R}{10^{18}\,\mathrm{cm}} \right)^{-1} \ \mathrm{G},$$

$$n_e = \eta \left(\frac{R}{10^{18}\,\mathrm{cm}} \right)^{-s} \ \mathrm{cm}^{-3}. \tag{2.1}$$

We find the normalization parameters ϕ and η by fitting GeV γ-ray data with our ALP-photon mixing model for different values of $s = 1$, 2 and 3.

To calculate the ALP-photon mixing effect for photons of energy ω propagating along the blazar jet, assumed z axis, we numerically solve the evolution equation [18, 16]

$$i\frac{d}{dz} \begin{pmatrix} A_\perp(z) \\ A_\parallel(z) \\ a(z) \end{pmatrix} = - \begin{pmatrix} \Delta_\perp \cos^2\xi + \Delta_\parallel \sin^2\xi & \cos\xi\sin\xi(\Delta_\parallel - \Delta_\perp) & \Delta_{a\gamma}\sin\xi \\ \cos\xi\sin\xi(\Delta_\parallel - \Delta_\perp) & \Delta_\perp \sin^2\xi + \Delta_\parallel \cos^2\xi & \Delta_{a\gamma}\cos\xi \\ \Delta_{a\gamma}\sin\xi & \Delta_{a\gamma}\cos\xi & \Delta_a \end{pmatrix} \begin{pmatrix} A_\perp(z) \\ A_\parallel(z) \\ a(z) \end{pmatrix}, \tag{2.2}$$

with an initial condition $(A_\perp, A_\parallel, 0)^t = (1/2, 1/2, 0)$ at $z \equiv R = 10^{18}$ cm, i.e., initially unpolarized photons. Here $A_\perp$ and $A_\parallel$ are the electromagnetic field components, respectively, perpendicular and parallel to B_T in the x-y plane. The ALP field is denoted with a. ξ is the angle the transverse magnetic field B_T makes with a fixed y axis in the x-y plane. For our calculation we fix it to $\pi/4$, and we will comment on variations of this angle in the following section. Other different terms in the ALP-photon mixing matrix, with the B_T and n_e given in Eq. (2.1), are $\Delta_\perp \equiv 2\Delta_{\mathrm{QED}} + \Delta_{\mathrm{pl}}$, $\Delta_\parallel \equiv (7/2)\Delta_{\mathrm{QED}} + \Delta_{\mathrm{pl}}$, and their reference values, following Refs. [18, 16], are given as

$$\Delta_{\mathrm{QED}} \equiv \frac{\alpha\omega}{45\pi} \left(\frac{B_T}{B_{\mathrm{cr}}} \right)^2 \simeq 1.34 \cdot 10^{-18} \phi^2 \left(\frac{\omega}{\mathrm{GeV}} \right) \left(\frac{R}{10^{18}\,\mathrm{cm}} \right)^{-2} \ \mathrm{cm}^{-1},$$

$$\Delta_{\mathrm{pl}} \equiv -\frac{\omega_{\mathrm{pl}}^2}{2\omega} \simeq -3.49 \cdot 10^{-26} \eta \left(\frac{\omega}{\mathrm{GeV}} \right)^{-1} \left(\frac{R}{10^{18}\,\mathrm{cm}} \right)^{-s} \ \mathrm{cm}^{-1},$$

$$\Delta_{a\gamma} \equiv \frac{1}{2} g_{a\gamma} B_T \simeq 1.50 \cdot 10^{-17} \phi \left(\frac{g_{a\gamma}}{10^{-10} \, \text{GeV}^{-1}} \right) \left(\frac{R}{10^{18} \, \text{cm}} \right)^{-1} \text{cm}^{-1},$$

$$\Delta_a \equiv -\frac{m_a^2}{2\omega} \simeq -2.53 \cdot 10^{-19} \left(\frac{\omega}{\text{GeV}} \right)^{-1} \left(\frac{m_a}{10^{-7} \, \text{eV}} \right)^2 \text{cm}^{-1}. \tag{2.3}$$

Here α is the fine structure constant and $B_{\text{cr}} = 4.414 \cdot 10^{13}$ G is the critical magnetic field. The plasma frequency is defined as $\omega_{\text{pl}} = \sqrt{4\pi\alpha n_e/m_e} = 3.713 \cdot 10^{-14} \sqrt{n_e/\text{cm}^{-3}}$ keV.

Although we do not assume a constant magnetic field or particle density in the ALP-photon mixing region, it is interesting to note that in such a constant B_T and n_e case the strong mixing of ALPs with $\gtrsim 1$ GeV photons take place for $B_T \sim 10^{-6}$–10^{-1} G and $n_e \sim 10^7$–10^8 cm^{-3} for $m_a \sim 10^{-7}$ eV and $g_{a\gamma} \sim 10^{-10}$ GeV^{-1} from the low and high critical-energy conditions $\omega_L \equiv |\omega_{\text{pl}}^2 - m_a^2|/2g_{a\gamma}B_T$ and $\omega_H \equiv 90\pi g_{a\gamma}B_{\text{cr}}^2/7\alpha B_T$, respectively [34, 18, 16]. For our case of varying B_T and n_e with R, however, transitions of photons to ALPs take place over different radii, $R \sim 10^{18}$–10^{21} cm for $\phi \sim 10^{-3}$ and $\eta \sim 10^9$ in Eq. (2.1). We assume a maximum radius of $R = 10^{22}$ cm to solve the evolution equation [Eq. (2.2)] numerically. We have checked that the ALP-photon mixing at larger radii does not contribute to the 0.1–400 GeV energy range of our interest.

3. Spectral fitting of 3C454.3 data and results

The 103 day observation, from 2010 September 1st to 2010 December 13th, of the blazar 3C454.3 by the *Fermi*-LAT [21] constitutes of 4 epochs: (i) An initial quiet or pre-flare period; (ii) A 13 day long plateau period; (iii) 5 day outburst or flare; and (iv) A post-flare period. Data points and upper limits of the γ-ray energy spectra ($\nu F_\nu \equiv E^2 \, dN/dE$) in these 4 epochs are shown in Fig. 1. To fit these data[3] with our ALP-photon mixing model, we assume an intrinsic single power-law spectrum for γ rays, $\propto E^{-\Gamma}$, at the production region. This spectrum is modified by a normalized suppression factor defined as

$$S(E) = 2 \left[|A_\parallel(E)|^2 + |A_\perp(E)|^2 \right], \tag{3.1}$$

where $A_\parallel(E)$ and $A_\perp(E)$ are the solutions of Eq. (2.2) with $\omega \equiv E(1+z)$ understood. The final observed energy spectrum is then

$$E^2 \, dN/dE = C E^{-\Gamma+2} S(E), \tag{3.2}$$

where C is measured in erg cm^{-2} s^{-1}.

Our ALP-photon mixing model for blazar jet has six free parameters: the normalizations for the jet magnetic field (ϕ) and electron density (η) [Eq. (2.1)]; ALP mass (m_a) and coupling ($g_{a\gamma}$); and the spectral parameters C and Γ. We let the two spectral parameters vary from epoch to epoch, as they are affected by the physical conditions at the γ-ray emission region at different times, but keep the other four (two environmental, ϕ and η; and two ALP properties, m_a and $g_{a\gamma}$) parameters fixed in all epochs as they are not affected by the γ-ray emission region. We repeat this for three different electron density profiles: $s = 1$, 2 and 3 in Eq. (2.1). The results of our fits are shown in Fig. 1 from the top to the bottom panels for the electron density profile $s = 3$ (a), 2 (b) and 1 (c), respectively.

---

[3]We do not fit the last data points in the flare or plateau epochs as they are absent in the quiet and post-flare epochs.
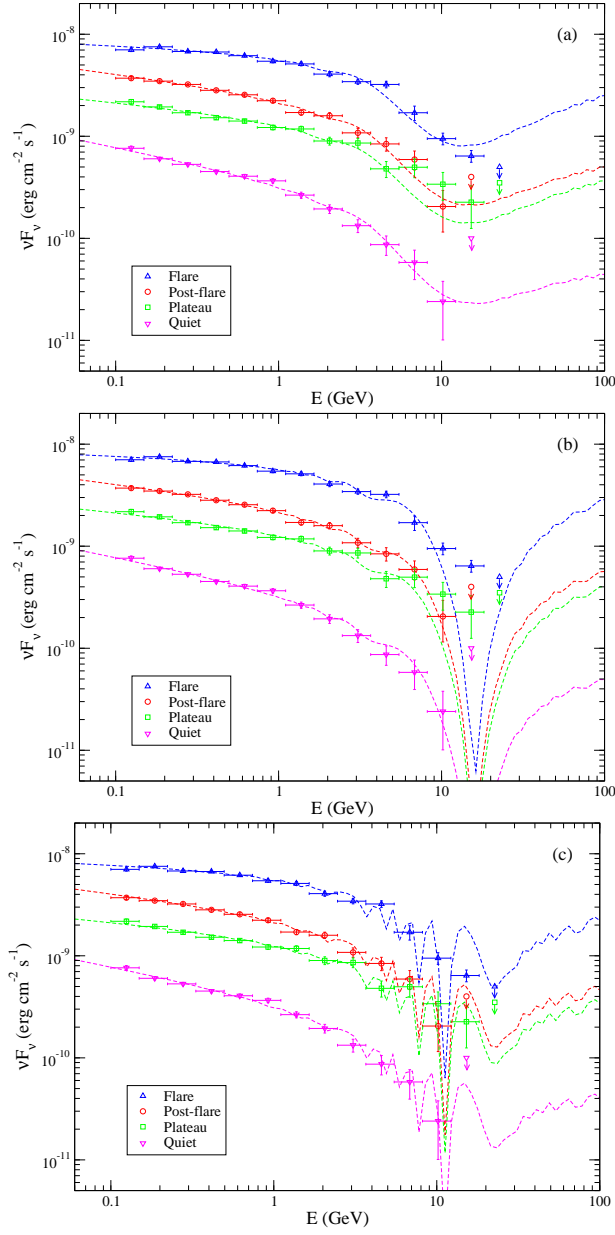
Figure 1: Fits to blazar 3C454.3 spectral data at 4 different epochs using ALP-photon mixing model in the blazar jet. Each plot is for a particular electron density profile n_e as a function of the jet radius R. The parameters m_a and $g_{a\gamma}$ are varied, but constrained to be the same at different epochs, together with the normalization and index of the production spectra, which are allowed to be different in different epochs. (a) Profile $n_e \propto R^{-3}$. Best-fit $m_a = 2.5 \cdot 10^{-7}$ eV and $g_{a\gamma} = 2.4 \cdot 10^{-10}$ GeV^{-1}. (b) Profile $n_e \propto R^{-2}$. Best-fit $m_a = 1.8 \cdot 10^{-7}$ eV and $g_{a\gamma} = 2.0 \cdot 10^{-10}$ GeV^{-1}. (c) Profile $n_e \propto R^{-1}$. Best-fit $m_a = 1.1 \cdot 10^{-7}$ eV and $g_{a\gamma} = 3.3 \cdot 10^{-10}$ GeV^{-1}. Note that we have not fitted the last data point in the Flare and Plateau epochs.

The $\chi^2_{\min}$ values and the best-fit spectral parameters for the case of $s = 3$ (Fig. 1 top panel) are: 24.5 (Flare, $C = 7.8 \cdot 10^{-9}$, $\Gamma = 2.07$); 9.8 (Post-flare, $C = 4.1 \cdot 10^{-9}$, $\Gamma = 2.21$); 15.5 (Plateau, $C = 2.1 \cdot 10^{-9}$, $\Gamma = 2.16$); and 11.0 (Quiet, $C = 7.8 \cdot 10^{-10}$, $\Gamma = 2.32$). The

best-fit environmental parameters are $\phi = 1.4 \cdot 10^{-2}$, $\eta = 2.0 \cdot 10^9$, and the best-fit ALP parameters are $m_a = 2.5 \cdot 10^{-7}$ eV, $g_{a\gamma} = 2.4 \cdot 10^{-10}$ GeV^{-1}.

In the case of the $s = 2$ electron density profile (Fig. 1 middle panel), the $\chi^2_{\min}$ values and the best-fit spectral parameters are: 23.3 (Flare, $C = 7.7 \cdot 10^{-9}$, $\Gamma = 2.06$); 4.3 (Post-flare, $C = 4.1 \cdot 10^{-9}$, $\Gamma = 2.20$); 17.0 (Plateau, $C = 2.1 \cdot 10^{-9}$, $\Gamma = 2.16$); and 10.2 (Quiet, $C = 7.8 \cdot 10^{-10}$, $\Gamma = 2.32$). The best-fit environmental parameters are $\phi = 1.6 \cdot 10^{-2}$, $\eta = 2.0 \cdot 10^9$, and the best-fit ALP parameters are $m_a = 1.8 \cdot 10^{-7}$ eV, $g_{a\gamma} = 2.0 \cdot 10^{-10}$ GeV^{-1}.

In the case of $s = 1$ electron density profile (Fig. 1 bottom panel) the $\chi^2_{\min}$ values and the best-fit spectral parameters are: 22.5 (Flare, $C = 8.0 \cdot 10^{-9}$, $\Gamma = 2.09$); 6.2 (Post-flare, $C = 4.2 \cdot 10^{-9}$, $\Gamma = 2.22$); 14.3 (Plateau, $C = 2.2 \cdot 10^{-9}$, $\Gamma = 2.18$); and 15.5 (Quiet, $C = 8.1 \cdot 10^{-10}$, $\Gamma = 2.34$). The best-fit environmental parameters are $\phi = 2.3 \cdot 10^{-2}$, $\eta = 2.2 \cdot 10^9$, and the best-fit ALP parameters are $m_a = 1.1 \cdot 10^{-7}$ eV, $g_{a\gamma} = 3.3 \cdot 10^{-10}$ GeV^{-1}.

Note that the total χ^2 values, summed over all of the four epochs, are comparable for the 3 electron density profiles that we have explored. There is a slight preference for the $s = 2$ profile. This is compatible with the density profile in the jet deduced from the reverberation measurement [30]. The ~ 10–20 mG magnetic field and the $\sim 2 \cdot 10^9$ cm^{-3} particle density at a radius $R \sim 10^{18}$ cm, just at the edge or outside the BLR, are also quite reasonable for the blazar jet. The intrinsic spectrum of γ rays varies between $\Gamma \sim 2.1$–2.3 and are compatible with the inverse Compton spectra by shock-accelerated electrons, as generally thought to be the emission mechanism of γ rays from blazars.

We can assess the significance of our results by adding up the χ^2 values for the four different epochs in each of the three possible cases $s = 1$, 2 and 3 and by comparing our results to the χ^2 resulting from a fit in which the probability of photon ALP transition is absent and therefore there are only two free spectral parameters C and Γ. For the model which provides the best fit to the data, that is, the $s = 2$ model, the $\chi^2_{\min,\text{ALP}}$ in the photon ALP mixing scenario is 54.8 for 48 spectral points and 24 free parameters, i.e. 24 degrees of freedom (dof). If we compute the χ^2 without the photon ALP transition we obtain $\chi^2_{\min} = 412.9$, we have again 48 spectral points to be fitted with 8 parameters, that is, 40 degrees of freedom. The difference in the fit for the two models, with and without photon ALP mixing, is $\Delta\chi^2_{s=2} = 358.1$ for $\Delta(\text{dof}) = 16$. The corresponding $p \simeq 0$ value is indicating that the ALP-photon mixing model fit the data much better than with just a simple spectrum characterized by Eq. (3.2), that is, the simple model can be rejected with a probability equal to 1 for practical purposes. For the $s = 1$ and $s = 3$ cases, $\Delta\chi^2_{s=1} = 354.4$ and $\Delta\chi^2_{s=3} = 352.1$ respectively and therefore $p \simeq 0$ also for these two cases.

The results quoted above have been obtained for the $\xi = \pi/4$, angle which describes the configuration of the transverse magnetic field B_T. Similar results could be obtained for different magnetic field configurations, although with slightly different best-fit values for the parameters describing the model.

Figure 2 shows 68% (yellow) and 95% (green) confidence-level regions in the m_a-$g_{a\gamma}$ parameter space for our ALP-photon mixing model for the γ-ray spectral data of the blazar 3C454.3. For these plots ($s = 3$, 2 and 1 for the left, middle and right panel, respectively) we have kept marginalized over the spectral parameters C and Γ as well as over the environmental parameters ϕ and η, i.e. the four parameters which are common

to all epochs. The best-fit points in the m_a-$g_{a\gamma}$ parameter space are denoted with a "∗" and these values are in agreement with the fits obtained in Fig. 1. Note that the allowed values for the ALP mass and its coupling depend rather weakly on the particle density profile in the blazar jet and are constrained in small ranges, $m_a \sim (0.8 - 2.5) \cdot 10^{-7}$ eV and $g_{a\gamma} \sim (1.2 - 3.3) \cdot 10^{-10}$ GeV.
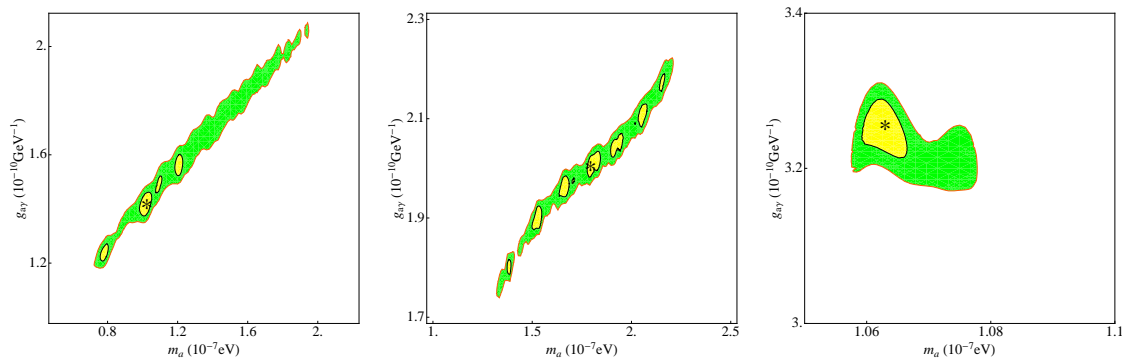

Figure 2: Contour plots of the 68% and 95% CL regions for the ALP mass and coupling in case of the electron density profiles in the jet (from left to right) $n_e \propto R^{-3}$, $n_e \propto R^{-2}$ and $n_e \propto R^{-1}$. The parameters of the production spectra for each epoch found in Fig. 1 are kept fixed. The position of the symbol "∗" denotes the best-fit point in the m_a-$g_{a\gamma}$ plane.

4. Consistency check with PKS1222+216 data

Fermi-LAT and MAGIC Cherenkov telescope made overlapping observations of PKS1222+216 on 2010 June 17 [22, 23]. During this time *Fermi*-LAT measured γ-ray emission in the ~ 0.3–1 GeV range and MAGIC measured VHE γ-ray emission in the ~ 70–400 GeV range. These data are showin in Fig. 3. VHE γ rays are subject to absorption due to $\gamma\gamma \rightarrow e^+e^-$ pair production with UV-infrared photons of the extragalactic background light (EBL). Figure 3 also shows the absorption corrected VHE "deabsorbed" spectrum as reported in Ref. [23] which used the EBL model in Ref. [31]. The EBL model in Refs. [32, 33] also gives very similar deabsorbed VHE spectrum.

Note that $\gtrsim 10$ GeV γ rays, if the emission region is well below the BLR, are also subject to absorption by BLR photons [37]. It was suggested in Ref. [15] that ALP-photon mixing in the BLR reduces the $\gamma\gamma$ optical depth as ALPs are not subject to absorption. The authors in Ref. [15] also fitted the high-energy and VHE spectra of PKS1222+216 using emissions, respectively, from two blobs and by assuming ALP-photon mixing in the BLR. The resulting ALP parameters are $m_a \sim 10^{-10}$ eV and $g_{a\gamma} \sim 1.4 \times 10^{-11}$. These are much different than our values from fitting multi-epoch 3C454.3 data, assuming that the γ-ray emission region is beyond BLR, in Sec. 3.

To verify that the ALP parameter values we have obtained are consistent with PKS1222+216 data, we have fitted the *Fermi*-LAT and MAGIC deabsorbed spectra assuming our simpler one-zone emission (in the form of a single power-law) region beyond the BLR. We have kept the m_a and $g_{a\gamma}$ values fixed for $s = 1$, 2 and 3 as in Fig. 1 but varied the environmental
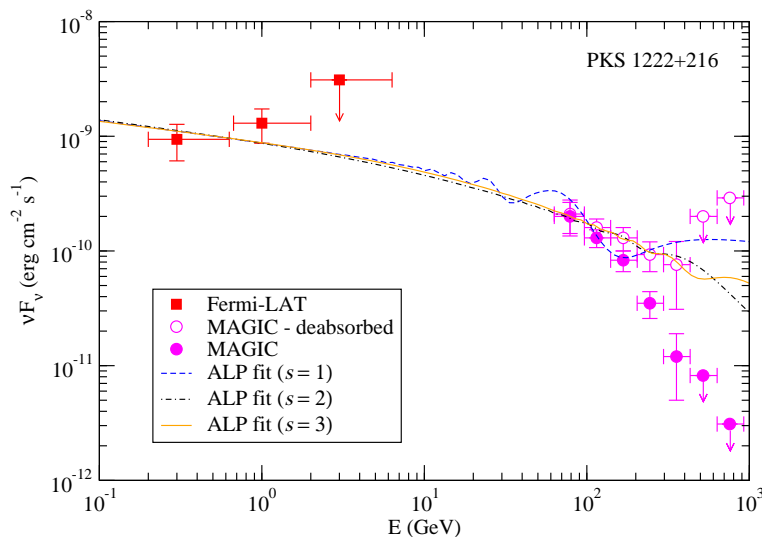
Figure 3: Blazar PKS1222+216 spectral data (filled symbols) from *Fermi*-LAT and MAGIC Cherenkov telescope. MAGIC-deabsorbed data points (empty symbols) correspond to EBL absorption corrected spectrum. The ALP model fits, for different electron density profiles $n_e \propto R^{-s}$, are performed using the *Fermi*-LAT and MAGIC deabsorbed data, while keeping m_a and $g_{a\gamma}$ values fixed for each s values as obtained in Fig. 1.

(ϕ, η) and spectral (C, Γ) parameters. The resulting fits with best-fit parameter values are shown in Fig. 3.

The $\chi^2_{\min}$ values and the best-fit environmental and spectral parameters for the case of $s = 3$ are: 1.3, $\phi = 6 \cdot 10^{-3}$, $\eta = 10^8$, $C = 1.4 \cdot 10^{-9}$ and $\Gamma = 2.17$. In case of $s = 2$, these values are: 1.5, $\phi = 6 \cdot 10^{-3}$, $\eta = 10^7$, $C = 1.4 \cdot 10^{-9}$ and $\Gamma = 2.19$. Finally in case of $s = 1$, these values are: 6.1, $\phi = 6 \cdot 10^{-3}$, $\eta = 2.4 \cdot 10^9$, $C = 1.4 \cdot 10^{-9}$ and $\Gamma = 2.19$. A single power-law fit without ALP mixing, on the hand, gives $\chi^2_{\min} = 3.4$. Except for the $s = 1$ case, the $\Delta\chi^2_{\min}$ for 2 dof difference are quite good. The parameter values are also quite reasonable for blazars.

5. Discussion and conclusions

The ALP mass, $m_a \sim (1-3) \cdot 10^{-7}$ eV, and coupling, $g_{a\gamma} \sim (1-3) \cdot 10^{-10}$ GeV^{-1}, that we have obtained from fitting spectral data of the well-studied blazar 3C454.3 in the GeV energy range, are just at the border of the exclusion zone in the m_a-$g_{a\gamma}$ parameter space from the Cern Axion Solar Telescope (CAST) experiment [10], as well as close to the region excluded by axion energy losses induced in massive stars [11] $g_{a\gamma} \lesssim (0.8-1) \cdot 10^{-10}$ GeV^{-1}. Note, however, that significant astrophysical model uncertainties might be present when deriving the former bound. Our results are also consistent with the recent exclusion region in the m_a-$g_{a\gamma}$ parameter space from the laboratory experiment of "Light Shining through a Wall" by the ALPS Collaboration [35]. A new generation of axion helioscopes [36] will be able to probe the parameter space which includes our best-fit m_a and $g_{a\gamma}$ values.

Interestingly the ALP mass that we have found in this work is very similar to the mass required to produce a spectral feature observed in the GRB data (in about 15% cases) through the similar ALP-photon mixing mechanism, but in a much shorter scale, $\sim 10^{13}$–10^{14} cm, jet with a much stronger, $\sim 10^4$–10^5 G, magnetic field [16]. On the other hand, our ALP mass is 3 orders of magnitude larger than the $\sim 10^{-10}$ eV mass suggested in Ref. [15] from modeling of > 10 GeV γ-ray data from PKS1222+216, assuming the γ-ray emission region is well below the BLR, contrary to our model. Moreover, ALP-photon mixing scenario was invoked in Ref. [15] to alleviate strong $\gamma\gamma$ absorption of VHE photons expected in the BLR rather than the direct flux suppression effect that we have explored. Using the same PKS1222+216 data we have obtained good fits for our ALP-photon mixing scenario for $m_a \sim 10^{-7}$ eV.

Very light, $\lesssim 10^{-10}$ eV, ALP mass is favored for mixing with VHE photons in the intergalactic magnetic field (IGMF) of megaparsec scale coherence length. Indeed for ~ 1 nG IGMF, $\sim 10^{-10}$ eV ALPs mix strongly with $\omega_L \sim 10\,(m_a/10^{-10}\,\text{eV})^2 (B_T/\text{nG})^{-1}$ GeV or higher energy photons, for $g_{a\gamma} \sim 10^{-10}$ GeV^{-1} and for typical particle densities of $n_e \sim 10^{-7}$ cm^{-3} in the intergalactic media. We calculate below the effect of IGMF on the $\sim 10^{-7}$ eV ALP mass that we have found.

The ALP-photon conversion probability in the IGMF can be written as (see, e.g., Ref. [16])

$$P_{a\gamma} = \sin^2 2\theta \sin^2\left(\frac{\Delta_{\text{osc}} L}{2}\right), \tag{5.1}$$

where $L \sim 1$ Mpc and the oscillation wave number and the mixing angle are given by $\Delta_{\text{osc}} = \sqrt{(\Delta_a - \Delta_\parallel)^2 + 4\Delta_{a\gamma}^2}$ and $\theta = (1/2)\arctan[2\Delta_{a\gamma}/(\Delta_\parallel - \Delta_a)]$, respectively. For our case of $m_a \sim 10^{-7}$ eV, $\Delta_{\text{osc}} \approx |\Delta_a|$, where Δ_a is given in Eq. (2.3), which is independent of any magnetic field. Since $L \gg \Delta_{\text{osc}}$, the oscillation term in Eq. (5.1) averages out. By requiring that the amplitude of oscillations be at least $1/2$ for ALPs from blazar 3C454.3 to be converted back to photons, we get $2\theta \approx \arctan(2\Delta_{a\gamma}/|\Delta_a|) \gtrsim \arcsin(1/\sqrt{2}) = \pi/4$. Thus the ALPs will convert back to photons for

$$B_{\text{IGMF}} \gtrsim 8.4 \cdot 10^{-3} \left(\frac{E}{\text{GeV}}\right)^{-1} \left(\frac{g_{a\gamma}}{10^{-10}\,\text{GeV}^{-1}}\right)^{-1} \left(\frac{m_a}{10^{-7}\,\text{eV}}\right)^2 \text{ G}. \tag{5.2}$$

This is already above any reasonable estimate of the IGMF, as well as the magnetic field in the clusters of galaxies. A similar analysis can be performed for the Galactic μG magnetic field. Thus the spectral feature in the ~ 1–10 GeV range for the blazar 3C454.3, due to conversions of photons to ALPs in the kpc scale jet, remains unchanged.

Explanations of the GeV spectral breaks seen in *Fermi*-LAT detected blazars without invoking new physics have been attempted earlier. These include $\gamma\gamma$ absorption of GeV photons by the Lyman line and continuum radiation from He II in the BLR [37], and two component GeV emission from Compton scattering of accretion disc photons and BLR photons [38]. While such scenarios can be responsible for the observed GeV spectral breaks, we note that in both scenarios the γ-ray emission region is below or within the BLR, contrary to our assumption. A future systematic study of GeV spectral breaks in all blazars will shed further light on the hints of ALP-photon mixing that we have found for

the blazar 3C454.3 and can provide clues to distinguish between a conventional and exotic explanation of the breaks in the blazar spectra.

6. Acknowledgments

References

[1] P. Sikivie, Phys. Rev. Lett. **51**, 1415 (1983) [Erratum-ibid. **52**, 695 (1984)].

[2] P. Sikivie, Phys. Rev. D **32**, 2988 (1985) [Erratum-ibid. D **36**, 974 (1987)].

[3] G. Raffelt and L. Stodolsky, Phys. Rev. D **37**, 1237 (1988).

[4] A. Ringwald, Phys. Dark Univ. **1**, 116 (2012) [arXiv:1210.5081 [hep-ph]].

[5] R. D. Peccei and H. R. Quinn, Phys. Rev. Lett. **38**, 1440 (1977).

[6] A. Arvanitaki, S. Dimopoulos, S. Dubovsky, N. Kaloper and J. March-Russell, Phys. Rev. D **81**, 123530 (2010) [arXiv:0905.4720 [hep-th]].

[7] B. S. Acharya, K. Bobkov and P. Kumar, JHEP **1011**, 105 (2010) [arXiv:1004.5138 [hep-th]].

[8] M. Cicoli, M. Goodsell, A. Ringwald, M. Goodsell and A. Ringwald, JHEP **1210**, 146 (2012) [arXiv:1206.0819 [hep-th]].

[9] A. Ringwald, arXiv:1209.2299 [hep-ph].

[10] S. Aune *et al.* [CAST Collaboration], Phys. Rev. Lett. **107**, 261302 (2011) [arXiv:1106.3919 [hep-ex]].

[11] A. Friedland, M. Giannotti and M. Wise, Phys. Rev. Lett. **110**, 061101 (2013) [arXiv:1210.1271 [hep-ph]].

[12] G. G. Raffelt and D. S. P. Dearborn, Phys. Rev. D **36**, 2211 (1987).

[13] R. Bhre, B. Dbrich, J. Dreyling-Eschweiler, S. Ghazaryan, R. Hodajerdi, D. Horns, F. Januschek and E. -A. Knabbe *et al.*, arXiv:1302.5647 [physics.ins-det].

[14] D. Hooper and P. D. Serpico, Phys. Rev. Lett. **99**, 231102 (2007) [arXiv:0706.3203 [hep-ph]].

[15] F. Tavecchio, M. Roncadelli, G. Galanti and G. Bonnoli, Phys. Rev. D **86**, 085036 (2012) [arXiv:1202.6529 [astro-ph.HE]].

[16] O. Mena, S. Razzaque and F. Villaescusa-Navarro, JCAP **1102**, 030 (2011) [arXiv:1101.1903 [astro-ph.HE]].

[17] M. A. Sanchez-Conde, D. Paneque, E. Bloom, F. Prada and A. Dominguez, Phys. Rev. D **79**, 123511 (2009) [arXiv:0905.3270 [astro-ph.CO]].

[18] N. Bassan, A. Mirizzi and M. Roncadelli, JCAP **1005**, 010 (2010) [arXiv:1001.5267 [astro-ph.HE]].

[19] D. Horns, L. Maccione, M. Meyer, A. Mirizzi, D. Montanino and M. Roncadelli, Phys. Rev. D **86**, 075024 (2012) [arXiv:1207.0776 [astro-ph.HE]].

[20] M. Simet, D. Hooper and P. D. Serpico, Phys. Rev. D **77**, 063001 (2008) [arXiv:0712.2825 [astro-ph]].

[21] A. A. Abdo, M. Ackermann, M. Ajello, A. Allafort, L. Baldini, J. Ballet, G. Barbiellini and D. Bastieri *et al.*, Astrophys. J. Lett. **733**, L26 (2011)

[22] Y. T. Tanaka, L. Stawarz, D. J. Thompson, F. D'Ammando, S. J. Fegan, B. Lott, D. L. Wood and C. C. Cheung *et al.*, Astrophys. J. **733**, 19 (2011) [arXiv:1101.5339 [astro-ph.HE]].

[23] J. Aleksic *et al.* [MAGIC Collaboration], Astrophys. J. **730**, L8 (2011) [arXiv:1101.4645 [astro-ph.HE]].

[24] F. Aharonian, Astrophys. J. **664**, L71 (2007) [arXiv:0706.0797 [astro-ph]].

[25] J. Albert, E. Aliu, H. Anderhub, P. Antoranz, A. Armada, C. Baixeras, J. A. Barrio and H. Bartko *et al.*, Astrophys. J. **669**, 862 (2007) [astro-ph/0702008].

[26] A. P. Marscher, S. G. Jorstad, F. D. D'Arcangelo, P. S. Smith, G. G. Williams, V. M. Larionov, H. Oh and A. R. Olmstead *et al.*, Nature **452**, 966 (2008).

[27] D. Giannios, D. A. Uzdensky and M. C. Begelman, Mon. Not. Royal Astron. Soc. Lett. **395**, L29 (2009) [arXiv:0901.1877 [astro-ph.HE]].

[28] M. C. Begelman, R. D. Blandford and M. J. Rees, Rev. Mod. Phys. **56**, 255 (1984).

[29] M. J. Rees, Mon. Not. Roy. Astron. Soc. **228**, 47 (1987).

[30] S. Kaspi and H. Netzer, Astrophys. J. **524**, 71 (1999)

[31] A. Dominguez, J. R. Primack, D. J. Rosario, F. Prada, R. C. Gilmore, S. M. Faber, D. C. Koo and R. S. Somerville *et al.*, Mon. Not. Royal Astron. Soc. **410**, 2556 (2011) [arXiv:1007.1459 [astro-ph.CO]].

[32] S. Razzaque, C. D. Dermer and J. D. Finke, Astrophys. J. **697**, 483 (2009) [arXiv:0807.4294 [astro-ph]].

[33] J. D. Finke, S. Razzaque and C. D. Dermer, Astrophys. J. **712**, 238 (2010) [arXiv:0905.1115 [astro-ph.HE]].

[34] A. De Angelis, O. Mansutti and M. Roncadelli, Phys. Lett. B **659**, 847 (2008) [arXiv:0707.2695 [astro-ph]].

[35] K. Ehret, M. Frede, S. Ghazaryan, M. Hildebrandt, E. -A. Knabbe, D. Kracht, A. Lindner and J. List *et al.*, Phys. Lett. B **689**, 149 (2010) [arXiv:1004.1313 [hep-ex]].

[36] I. G. Irastorza, F. T. Avignone, S. Caspi, J. M. Carmona, T. Dafni, M. Davenport, A. Dudarev and G. Fanourakis *et al.*, JCAP **1106**, 013 (2011) [arXiv:1103.5334 [hep-ex]].

[37] J. Poutanen and B. Stern, Astrophys. J. **717**, L118 (2010) [arXiv:1005.3792 [astro-ph.HE]].

[38] J. D. Finke and C. D. Dermer, Astrophys. J. **714**, L303 (2010) [arXiv:1004.1418 [astro-ph.HE]].